Rapid Biphasic Decay of Intact and Defective HIV DNA Reservoir During Acute Treated HIV Disease

Alton Barbehenn[1], Lei Shi[2], Junzhe Shao[2], Rebecca Hoh[1], Heather M. Hartig[1], Vivian Pae[1], Sannidhi Sarvadhavabhatla[1], Sophia Donaire[1], Caroline Sheikhzadeh[1], Jeffrey Milush[5], Gregory M. Laird[3], Mignot Mathias[3], Kristen Ritter[3], Michael J. Peluso[1], Jeffrey Martin[4], Frederick Hecht[1], Christopher Pilcher[1], Stephanie E. Cohen[1,6], Susan Buchbinder[6], Diane Havlir[1], Monica Gandhi[1], Timothy J. Henrich[5], Hiroyu Hatano[1], Jingshen Wang[2], Steven G. Deeks[1], and Sulggi A. Lee*[1]

[1]Department of Medicine, Division of HIV, Infectious Diseases & Global Medicine, University of California San Francisco, San Francisco, CA 94110, USA. [2]Department of Biostatistics, University of California Berkeley, Berkeley, CA 94110, USA. [3]AccelevirDiagnostics, Baltimore, MD 21202, USA. [4]Department of Biostatistics & Epidemiology, University of California San Francisco, CA 94158, USA. [5]Department of Medicine, Division of Experimental Medicine, University of California San Francisco, San Francisco, CA 94110, USA. [6]San Francisco Department of Public Health, San Francisco, CA 94102, USA.

[#]Co-Lead Authors: Alton Barbehenn and Lei Shi

[*]Corresponding Author: sulggi.lee@ucsf.edu

ABSTRACT

Despite antiretroviral therapy (ART), HIV persists in latently-infected cells ("the reservoir") which decay slowly over time. Here, leveraging >500 longitudinal samples from 67 people with HIV (PWH) treated during acute infection, we developed a novel mathematical model to predict reservoir decay from peripheral CD4+ T cells. Nonlinear generalized additive models demonstrated rapid biphasic decay of intact DNA (week 0-5: $t_{1/2}$~2.83 weeks; week 5-24: $t_{1/2}$~15.4 weeks) that extended out to 1 year. These estimates were ~5-fold faster than prior decay estimates among chronic treated PWH. Defective DNA had a similar biphasic pattern, but data were more variable. Predicted intact and defective decay rates were faster for PWH with earlier timing of ART initiation, higher initial CD4+ T cell count, and lower pre-ART viral load. These data add to our limited understanding of HIV reservoir decay at the time of ART initiation, informing future curative strategies targeting this critical time.

Abstract Word Count (limit 150): 148

Title Word Count (max 15): 15

Manuscript Word Count (5,000; Methods 3,000 words): 4,938

Keywords: acute HIV; antiretroviral therapy (ART); HIV reservoir decay; pre-exposure prophylaxis (PrEP)

CONFLICTS: The authors do not have a commercial or other association that might pose a conflict of interest.

FUNDING: This work was supported in part by the National Institutes of Health: K23GM112526 (SAL), the DARE Collaboratory (UM1AI164560; SGD), the AccelevirDx HIV Reservoir Testing Resource (U24AI143502; GML), and NIH/NIAID R01A141003 (TJH). This work was also supported by the amfAR Research Consortium on HIV Eradication a.k.a. ARCHE (108072-50-RGRL; SGD), the Bill & Melinda Gates Foundation (INV-002703; SGD), and investigator-initiated research grants from ViiV Healthcare (A126326; SAL) and Gilead Sciences (IN-US-236-1354; SAL). The content of this publication does not necessarily reflect the views or policies of the Department of Health and Human Services, the San Francisco Department of Health, nor does mention of trade names, commercial products, or organizations imply endorsement by the U.S. Government. The funders had no role in study design, data collection and analysis, decision to publish, or preparation of the manuscript.

Previous presentation: Preliminary data were presented in July 2023, as a poster presentation at the International AIDS Society (IAS) conference in Brisbane, Australia.

Reprints: Reprint requests can be directed to Dr. Sulggi Lee, the corresponding author (contact information above).

Acknowledgements:

The authors wish to acknowledge the participation of all the study participants who contributed to this work as well as the clinical research staff of the UCSF Treat Acute HIV and SCOPE

cohorts who made this research possible. All funders had no role in study design, data collection and analysis, decision to publish, or preparation of the manuscript. All authors provided critical feedback in finalizing the report. SGD, HH, and SAL conceived and designed the study. SGD, HH, and SAL obtained funding to support the clinical enrollment of study participants, and SAL and SGD obtained funding to support characterization of the HIV reservoir. SEC, SB, DH, and MG facilitated coordination with San Francisco Department of Public Health and Ward 86 clinical services to link patients into care and provided critical feedback on the clinical management of acute HIV. SAL, RH, SGD, TJH, HMH, SS, SD, and VP coordinated the collection, management, and quality control processes for the clinical data, and SAL, SGD, JM, FH, and CP provided biospecimens. JM and TJH performed biospecimen processing, GML, MM, and KR performed the HIV reservoir assays. LS developed the initial decay models, under the guidance of SAL and JW, and AB and SAL further modified these models under the guidance of JW, LS, and JS. GML, MM, KR, LS, JS, JW, and SAL analyzed the HIV reservoir data. AB, SAL, LS, JS, JW, SS, SD, VP, and CS performed data visualization for the manuscript. SAL and AB wrote the report with critical feedback from LS, JW, and the additional authors.

INTRODUCTION

While antiretroviral therapy (ART) is able to suppress virus to undetectable levels, virus rapidly rebounds from latently-infected cells ("the HIV reservoir") within weeks of ART interruption and is thus, not a cure.[1-8] Thus, a major goal is to eradicate and/or accelerate the decay of the reservoir in order to achieve clinical remission. However, HIV cure trials to date have largely failed to demonstrate a clinically meaningful reduction in the size of the HIV reservoir and/or lead to sustained ART-free remission.[9-12] The majority of these trials have included people with HIV (PWH) treated during chronic infection long after reservoir establishment (i.e., several years after initiating ART).[13-18] Recent combination trials (e.g., broadly neutralizing antibodies given with ART) have yielded more promising results, and a few participants have demonstrated extended post-intervention viral control,[19-21] but the mechanisms by which these participants have enhanced viral control remain unclear.

Individuals who initiate ART "earlier" (<6 months after infection) are more likely to become "post-treatment controllers" (PTCs), demonstrating ART-free viral control after a period of initial ART suppression.[22] PWH treated during chronic HIV often have larger reservoirs[23-30] and exhausted/dysfunctional immune responses[31-33] (due to prolonged periods of untreated HIV infection). Thus, different host factors, such as timing of ART initiation, initial CD4+ T cell count, or pre-ART HIV viral load, may have profound impact on HIV reservoir decay rates, and yet there are limited reservoir decay modeling studies accounting for these factors. While there have now been a handful of studies modeling how quickly the HIV reservoir decays during prolonged ART (~20 years),[34-37] there have been fewer studies modeling decay rates after acute treated HIV,[38-40] and none directly performing mathematical modeling of HIV intact and defective DNA decay.

Here, leveraging >500 longitudinal blood samples, we developed a novel mathematical model of reservoir decay among 67 participants from the UCSF Treat Acute HIV cohort initiating ART <100 days of HIV infection.[41] We fit various mono-, bi-, and triphasic decay curves for both

HIV "intact" (infected cells harboring intact viral sequences able to produce infectious virions) and "defective" (the majority of the HIV reservoir but incapable of producing infectious virions) DNA, and we observed biphasic decay patterns for both measures. Furthermore, both HIV intact and defective DNA decay rates were significantly faster among PWH with known clinical factors associated with enhanced host viral control: higher initial CD4+ T cell count, earlier initiation of ART, and lower pre-ART viral loads.[23,24,34,42,43] As further validation of our mathematically modeling approach, we also fit decay models for plasma HIV RNA ("viral load" measured at each study visit using a standard clinical assay with limit of detection < 40 copies/mL). We observed a triphasic decay of plasma HIV RNA, similar to prior reports among PWH initiating ART.[3,4,40] Our data are the first to our knowledge to describe a predictive mathematical model quantifying decay rates of HIV intact and defective DNA during acute treated HIV.

RESULTS

Characteristics of study participants

A total of 67 adults (83% of those screened) with a new diagnosis of acute HIV (<100 days between HIV infection to ART initiation date) were included in the study (**Table 1, Supplementary Fig. 1**).[44] All 67 participants completed monthly follow-up visits in the study for the full 24 weeks. A large proportion (65.7%) of participants were co-enrolled in our longitudinal UCSF SCOPE HIV cohort and remained in study beyond 24 weeks, with study visits approximately every 3-4 months. The median follow-up for our cohort was 0.81 (interquartile range = 0.47-1.66) years. We calculated the estimated date of detected infection (EDDI) for each participant using an algorithm[45,46] successfully applied to other acute HIV cohorts[38,39] (**Supplementary Fig. 2**). We also estimated Fiebig stage[47,48] for each participant, an older but often cited method for staging recency of HIV infection (**Fig. 1**). Consistent with our San Francisco-based study population, participants were mostly male (97%) and reflected local and

national racial/ethnic trends of higher incident acute HIV in these populations (**Fig. 1**).[49] Baseline study visit HIV-1 antigen/antibody (Architect) and HIV-1 antibody (Geenius) testing demonstrated 27% and 28% false negative/indeterminate rates (**Supplementary Fig. 3**), respectively, consistent with our San Francisco Department of Public Health (SFDPH) reported estimates for new acute HIV diagnoses.[50] Genotype data (Monogram) were available for a subset of 57 participants; 77% had wild-type HIV, 9% had M184V/I mutations (all were reported among participants citing prior and/or current pre-exposure prophylaxis [PrEP] use), and 14% had evidence of possible partner-transmitted resistance mutations (based on referral of newly diagnosed partners within our cohort and/or SFDPH partner tracing[50]).

Our cohort also reflected a high proportion of self-reported prior PrEP use (42% ever use, 20% use in the past 10 days), reflecting San Francisco's early and widespread adoption of PrEP.[50] All PrEP reported in this study was oral PrEP with tenofovir disoproxil fumarate/emtricitabine (TDF/FTC), as this was the only form clinically available during the study period. Among individuals reporting overlapping PrEP use within 10 days of their EDDI, six participants had probable HIV acquisition while on PrEP (median baseline $\log_{10}$HIV RNA = 2.2 copies/mL, ~3 $\log_{10}$ lower than those not reporting PrEP overlap) (**Table 1, Supplementary Fig. 4**), including one participant[51] who may have acquired HIV in the setting of therapeutic PrEP concentrations (confirmed by plasma and hair ART concentrations).

Rapid biphasic decay of HIV intact and defective DNA

Overall, after fitting various mono-, bi-, and triphasic decay curves using semiparametric generalized additive models, we found that a biphasic decay pattern with an inflection point (τ) = week 5 best fit the data for HIV intact and defective DNA (**Figs. 2-3, Supplementary Fig. 5**). Validation of these models against the observed data showed good model performance (**Fig. 4, Supplementary Figs. 6-7**) and that HIV intact and defective DNA decay patterns significantly

predicted faster decay rates (**Figs. 5-6**) for participants with known clinical factors associated with smaller HIV reservoir size.[23,24,34,42,43]

First, we modeled HIV intact and defective DNA using a linear effect of time on ART (which assumes a constant rate of change regardless of the duration of viral suppression). However, since we observed evidence of nonlinearity, we fit nonlinear generalized additive models to better estimate HIV intact and defective DNA decay patterns. For all models, we tested clinical factors of age, pre-ART CD4+ T cell count, pre-ART viral load, and timing of ART initiation for inclusion as potential covariates. We found that both HIV intact and effective DNA were well described by a biphasic model, comparing Akaike information criteria (AIC) (**Fig. 2a**) and thus was chosen over a triphasic model since comparing the minimum predicted mean absolute error (MAE) using leave-one-out cross-validation and/or the minimum predicted mean squared error (MSE) (**Fig. 2b**), suggested similar inflection points. For HIV intact DNA, the first and second inflection points were similar, suggesting that a single inflection point – i.e., a biphasic model – adequately described the data, and for HIV defective DNA, since the first inflection point was close to zero, this again suggested that a biphasic model well described the data. We then further determined that the inflection point of τ =5 weeks, after comparing MAEs and MSEs, was optimal for both HIV intact and defective DNA (**Fig. 3, Supplementary Fig. 5**). Since we found that several key clinical factors (previously associated with HIV reservoir size initiation[23,24,34,42,43]) were strongly associated with HIV DNA decay rates (**Figs. 5-6**), all final models included terms for initial CD4+ T cell count, pre-ART viral load, and timing of ART initiation.

Our final biphasic decay model of HIV intact DNA demonstrated a rapid $t_{1/2}$~2.83 (95%CI = 2.39-3.27) weeks for the first ~5 weeks of AR, followed by a slower second decay phase with a $t_{1/2}$~15.4 (95%CI = 12.0-21.9) weeks (**Supplementary Table 1**). HIV defective DNA had a similar pattern, with an initial rapid decay ($t_{1/2}$~1.36, 95%CI = 1.17-1.55 weeks), followed by a slower decay, but the change in decay was not statistically significantly given the large

variability in HIV defective DNA during this second phase (**Fig. 4**). Interestingly, we observed a significantly faster decay of HIV defective vs. intact DNA during the first phase (p<1e-16) (**Fig. 4**). While the reasons for this are unclear, given the frequency of our sampling at these acute HIV timepoints, our observation may potentially be due to (1) a true biological phenomenon uniquely captured by our frequent early sampling and/or (2) reflect unique properties of the IPDA (see **Discussion**).

Our final models also demonstrated significantly faster decay rates with clinical factors associated with smaller reservoir size (**Figs. 5-6**). For example, our models estimated that for HIV intact DNA, for each week earlier that ART was initiated, the $t_{1/2}$ was predicted to be reduced by ~0.0827 (95%CI = 0.0203-0.145) and by ~1.08 (95%CI = 0.316-1.84) during the second phase (**Supplementary Table 3**). Similarly, our models predicted that higher initial CD4+ T count and lower pre-ART HIV RNA predicted significantly faster HIV intact and defective decay rates (**Supplementary Table 4**). Further validation using fitted spline models again demonstrated that higher initial CD4+ T count and lower pre-ART HIV RNA predicted faster HIV intact and defective DNA decay rates (**Supplementary Fig. 10**). For example, a participant with an initial CD4+ T cell count of 900 cells/mm^3 was predicted to have ~10 times faster decay of HIV intact DNA than a participant with an initial CD4+ T cell count of 300 cells/mm^3. Similar patterns were observed for HIV defective DNA, but the fitted splines were less linear.

While were unable to perform adjusted analyses for other important clinical factors such as gender and race/ethnicity given the small sample sizes in our study (**Table 1**), we did perform sensitivity analyses focusing on the small number of cisgender and transgender women, as well as the small numbers of PWH reporting PrEP use within 10 days of HIV diagnosis. These analyses demonstrated that results were overall relatively unchanged and that these participants did not necessarily fall in the lower range of reservoir measurements (**Supplementary Fig. 8**). Furthermore, to ensure that the selected inflection point of τ = 5 weeks

was not influenced by potential outlier data, we performed three different sensitivity analyses excluding participants for whom HIV reservoir measures might fall on the higher and/or lower range of values: (1) individuals reporting prior PrEP use within 10 days of HIV infection, (2) participants with plasma viral load "blips" (defined as a one-time viral load >1000 copies/mL or two consecutive viral loads >100 copies/mL between weeks 0-24), and (3) participants with sudden increases in HIV intact DNA (defined as >50% increase between two consecutive measurements during weeks 0-24). These sensitivity analyses demonstrated that τ = 5 weeks remained a reasonable choice for the model's inflection point (**Supplementary Fig. 9**) and that the estimates were overall unchanged after exclusion (**Supplementary Table 2**).

Triphasic decay of plasma HIV RNA

As further validation of our mathematical modeling approach, we also fit decay models for plasma HIV RNA. Plasma HIV RNA ("viral load") was measured at each study visit using a standard clinical assay (Abbott Real Time PCR assay, limit of detection < 40 copies/mL). We again fit various mono-, bi-, and triphasic models, and a triphasic decay model best fit these data with inflection points at 0.5 and 4 weeks (**Supplementary Fig. 11**). Our findings are consistent with prior published work describing triphasic decay of plasma HIV RNA in treatment naïve PWH initiating integrase inhibitor-based therapy.[52] Our final adjusted models predicted a rapid initial decay ($t_{1/2}$ ~0.659, 95% CI = 0.541-0.778 days), a second decay ($t_{1/2}$ ~4.93, 95% CI = 3.98-5.89 days), with no significant decay during the third phase (**Supplementary Table 5**), closely mirroring prior reported estimates describing a $t_{1/2}$= 1.14, 9.19, and 340 days, respectively.[52] As expected, we observed that the majority of our cohort had undetectable plasma viremia by a median of 4.14 weeks, consistent with viral suppression rates among treatment naïve PWH initiating integrase inhibitor-based ART.[53,54] Similar to our approach used for our HIV DNA decay models, we validated our final triphasic plasma HIV RNA decay model by comparing predicted vs. observed values and found that the model produced unbiased

231 estimates across a range of plasma HIV RNA values (**Supplementary Fig. 12**). We again found
232 that known clinical factors associated with reservoir size –e.g., initial CD4+ T cell count and
233 earlier timing of ART initiation –were also associated with accelerated decay rates
234 (**Supplementary Figs. 13-15**).
235
236 **DISCUSSION**
237 Leveraging >500 longitudinal blood samples from the UCSF Treat Acute HIV cohort, we
238 performed mathematical modeling and demonstrated a rapid biphasic decay of HIV intact and
239 defective DNA. Our estimates for HIV intact DNA decay were significantly faster (~5-fold)
240 compared to prior estimates from chronic treated[3] PWH initiating ART. Furthermore, clinical
241 factors associated with smaller HIV reservoir sizes (e.g., earlier timing of ART initiation, higher
242 initial CD4+ T cell count, and lower pre-ART viral load) predicted faster decay rates of both HIV
243 intact and defective DNA. We further validated our modelling approach by fitting plasma HIV
244 RNA decay rates, and we observed a triphasic decay pattern, consistent with prior estimates.[52]
245 Our mathematical modeling approach may serve as a meaningful way to predict expected
246 decay rates after ART initiation and the potential impact of clinical factors that may differ when
247 comparing across global HIV cohorts that may also have different host genetics, HIV-1
248 subtypes, etc. This approach may also help inform the design of future HIV cure trials, e.g., to
249 predict optimal timeframes during which an intervention may have the greatest impact on
250 accelerating reservoir decay and/or limiting reservoir establishment.
251 Our findings compare to several key prior modeling studies of HIV reservoir decay,[3,55-58]
252 all of which fit mostly unadjusted fully parameterized mixed effects models but still lend support
253 to our findings. For example, we observed an initial rapid HIV intact DNA decay rate of $t_{1/2}$ of
254 ~2.83 weeks (~0.71 months), followed by a slower second phase with a $t_{1/2}$ ~15.4 weeks (~3.9
255 months). Strikingly, this first phase decay estimate is nearly identical to prior reports in chronic
256 treated PWH initiating ART ($t_{1/2}$ = 0.43 months),[3] but our estimates for the second phase of

decay were ~5-fold faster than estimates from this other study ($t_{1/2}$ = 19 months), well below their confidence limits (8.23-43.7 months).[3] Our faster rate of HIV intact DNA decay during this second phase are unclear but may potentially be due to true biological differences (e.g., less exhausted immune cells compared to chronic treated PWH[59,60]) or reflect greater precision in estimating decay rates from our frequent sampling (every 2-4 weeks). The initial rapid decay of HIV-infected cells after ART initiation is thought to be largely due to clearance of free virions and death of productively infected cells.[3,4,52,61,62] We estimated similar first phase decay rates as those previously reported in chronic treated PWH initiating ART,[3] suggesting that death of productively infected cells, regardless of timing of ART initiation, may indeed be driving the first phase decay estimates. Furthermore, plasma (cell-free) HIV RNA correlates with the frequency of productively infected CD4+ T cells;[63] our plasma HIV RNA decay estimates provide further support as these estimates are again consistent with prior reported clearance rates of productively infected CD4+ T cells ($t_{1/2}$ ~ 0.7 days).[64] Meanwhile, the second phase of reservoir decay after ART initiation is thought to represent a "contraction phase" when activated cells transition from an effector to a memory phenotype with ART-mediated antigen reduction.[65-67] This second phase is thought to be largely driven by death of longer-lived memory cells.[68,69] Indeed, if we extrapolate the second phase of our HIV intact DNA model, we estimate that PWH who delay ART initiation to ~56 weeks after HIV infection have a predicted $t_{1/2}$ that is comparable to the (slower) second phase decay reported in chronic treated PWH.[3] Our data suggests that – especially during this second phase of decay – that curative interventions given during this critical window of time may have the potential to significantly reduce the establishment of these long-lived memory cells.

Our data are also consistent with findings from two prior acute HIV cohorts[38,58] that did not measure IPDA (HIV intact and defective DNA) but did measure HIV total, integrated DNA, and 2-LTR DNA by real-time PCR[70] and also performed the quantitative viral outgrowth (QVOA[25,68,71]) and multiply spliced tat/rev (TILDA[72]) assays. One of these studies by Massanella

and colleagues performed mathematical modeling and also demonstrated biphasic decays of HIV total, integrated, and 2-LTR DNA, with a similar inflection point (6 weeks).[58] While they were unable to report decay models for QVOA or TILDA (likely due to the low frequency of HIV-infected cells despite the large number of input cells,[73,74] which may have precluded more complex decay modeling), their estimates for HIV total, integrated, and 2-LTR decay rates closely compare to our estimates for defective DNA. The population of HIV-infected cells generally falls into three broad categories: (1) truly "intact" proviruses, (2) "partially defective" proviruses that can produce defective HIV RNA/proteins, which, despite being unable to produce virus, can still lead to immunogenic/cytopathic effects,[75] and (3) truly "inert" proviruses that express no HIV RNA or proteins. While the assays in this other study did not specifically discriminate intact from defective viral sequences, since the majority of the HIV reservoir consists of defective provirus[73] and since the majority of infected cells in acute PWH consist of these highly unstable unintegrated linear HIV DNA (with an estimated half-life of ~2 days),[76] the overlap in our modeling results may suggest an overlap in the population of HIV-infected cells captured by our respective assays.

Finally, it is important to note that the decay rates described here are likely complementary to, but not the same as, decay rates described in several long-term ART studies.[34-37,71,77] First, these long-term ART studies (in chronic treated PWH) did not sample participants at the time of ART initiation and had less frequent sampling over longer periods of ART suppression.[34-36,57] Overall, these studies described a biphasic decay (inflection point ~7 years of ART) with a $t_{1/2}$ ~44 months for HIV intact DNA[71,77] and found that HIV intact DNA decayed faster than defective DNA, presumably due to preferential clearance of intact, or "replication-competent", provirus during long-term ART.[34-36,57,78,79] However, HIV intact DNA decay rates have also been shown to plateau or even an increase in some individuals during prolonged ART.[36,57] Our biphasic model identified a somewhat surprising finding that HIV defective DNA decayed faster than HIV intact DNA during the first phase. The reasons for this

are unclear but may reflect true biological phenomena uniquely captured by our frequent early sampling and/or unique properties of the IPDA. Since the majority of the HIV reservoir consists of defective provirus,[73] estimates of HIV total, integrated, and 2-LTR DNA decay rates from the study by Massanella et. al., ($t_{1/2}$ = 14.5, 14.1, and 30.5 days, respectively[58]) are largely consistent with our estimates of defective DNA decay rates ($t_{1/2}$ =9.5 days) during the first phase of decay, suggesting a potential true biological phenomena that warrants further study. Alternatively, a second possibility is that our observations reflect some misclassification of HIV "intact" provirus (i.e., since the IPDA targets just two regions of the HIV genome to define "defective" provirus[80]). However, Reeves and colleagues recently performed detailed validation experiments (e.g., using quantitative viral outgrowth assay and near full-length sequencing) and showed that the rate of misclassification is <5% with the IPDA,[55] suggesting that this degree of misclassification alone would be unlikely to fully explain our findings.

Our study has several limitations that deserve mention. While we leveraged several hundred longitudinal blood samples from acute treated PWH, we did not model the HIV tissue reservoir; our tissue studies are currently underway but will be limited in the number of longitudinal timepoints to perform similar detailed modeling. Since the peripheral HIV reservoir largely reflects proviruses originating from the tissue reservoir,[38,81-83] tissue reservoir decay estimates in ours as well as other studies should be modeled in parallel with the more frequently sampled peripheral reservoir decay estimates in future work. We performed IPDA, which, while highly scalable for a large number of samples, less accurately quantifies the replication-competent reservoir compared to near-full length proviral sequencing or QVOA. Nonetheless, HIV intact DNA measured by IPDA closely reflect results from these other assays, even considering the known enrichment of integrated forms of HIV DNA observed in acute PWH.[38] As with all molecular assays for HIV, certain polymorphisms at primer or probe binding sites can impact IPDA assay performance. We observed IPDA signal failure for 6 participants (8.9%) – a rate consistent reports from large HIV cohorts from North America and Europe where subtype B

predominates (6-7%).[34,84] We also did not measure changes in clonal landscape (e.g., HIV integration). The clonal landscape at the time of acute HIV is extremely diverse, and we hypothesize that this effect is more likely to have greater higher impact after longer duration of ART suppression. Future models should include these parameters to formally test this hypothesis. Finally, there are few highly characterized acute HIV cohorts to date, and each study possesses unique host and viral characteristics making direct cross-cohort comparisons challenging. Our study included mostly men who have sex with men and HIV-1 subtype B. It will be critical to validate our HIV reservoir decay models in global populations with distinct host genetic ancestry, HIV-1 subtypes, and clinical features to facilitate cross-cohort comparisons and inform future HIV cure trial design and interpretation.

The long-lived latent reservoir is a key defining target for HIV cure, but how and where these cells then become “the long-lasting latent reservoir” remains unclear. Even in reservoir decay studies analyzing data out to 20 years of ART suppression, decay patterns are not broadly generalizable.[36,57] Thus, there is a critical need for a scalable approach to broaden our understanding of HIV reservoir decay patterns across a global population of PWH, ideally aligning study designs and assays and performing meta-analyses, including how key clinical factors such as the timing of ART initiation, initial CD4+ T cell count, and pre-ART viral load influence decay rates.

METHODS

Study participants

Individuals with newly diagnosed acute (<100 days) from HIV infection were enrolled in the UCSF Treat Acute HIV cohort between December 1, 2015 to November 30, 2020 and co-enrolled in the UCSF SCOPE HIV cohort, an ongoing longitudinal study of over 2,500 PWH. Eligible participants were provided same-day ART initiation with tenofovir/emtricitabine

(TDF/FTC, then TAF/FTC once available in 2016) + dolutegravir (DTG) and linked to clinical care.[50] Individuals reporting concomitant PrEP use (<100 days from any potential exposure to HIV by history and/or clinical test results) were also started on darunavir+ritonavir (DRV/r) as a fourth drug, which was continued until confirmation of baseline HIV genotyping test results (Monogram Biosciences, South San Francisco, CA, U.S.A.). Additional ART changes necessary for clinical care (e.g., laboratory abnormalities, drug-drug interactions, and/or participant preference) were honored and adjusted during the period of study. Participants signed a release of information which allowed clinical data extraction to determine prior HIV negative test results from the SFDPH, as well as additional HIV test results.

Study participants were seen for monthly study visits for the first 24 weeks (including an additional week 2 visit to confirm HIV test results from baseline visit) and then every 3-4 months thereafter. Inclusion criteria for the study were prior HIV negative testing within the last 90 days, laboratory-confirmed HIV-1 infection by antibody/antigen and/or plasma HIV RNA assay, and willingness to be participate in the study for at least 24 weeks. Participants with severe renal or hepatic impairment, concurrent treatment with immunomodulatory drugs, or exposure to any immunomodulatory drugs in the preceding 90 days prior to study entry, pregnant or breastfeeding women, or participants unwilling to agree to the use a double-barrier method of contraception throughout the study period, were excluded. For each study participant, the estimated date of detected HIV infection (EDDI) was calculated using the Infection Dating Tool (https://tools.incidence-estimation.org/idt/).[45] At each visit, detailed interviews included questions regarding current medications, medication adherence, intercurrent illnesses, and hospitalizations were performed. In addition, peripheral blood sampling at each visit was performed to measure plasma HIV RNA (Abbott Real Time PCR assay, limit of detection <40 copies/mL), CD4+ T cell count, and clinical labs (complete blood count, metabolic panel). All

participants provided written informed consent, and the institutional review board of UCSF approved the research.

HIV reservoir quantification

The frequencies of HIV intact and defective (3' and 5') DNA were quantified using the intact proviral DNA assay (IPDA).[85] CD4+ T cells were isolated from cryopreserved PBMCs (EasySep Human CD4+ T cell Enrichment Kit, Stemcell Technologies), with cell count, viability, and purity assessed by flow cytometry. Negatively selected CD4+ T cells were recovered (median cells = $2x10^6$ with median viability = 97%) and genomic DNA extracted using the QIAamp DNA Mini Kit (Qiagen). DNA concentration and quality were determined by fluorometry (Qubit dsDNA BR Assay Kit, Thermo Fisher Scientific) and ultraviolet-visible (UV/VIS) spectrophotometry (QIAxpert, Qiagen). The frequency of intact provirus was determined using two multiplex digital droplet polymerase chain reaction (ddPCR) assays performed in parallel: (1) the HIV-1 Proviral Discrimination reaction which distinguishes intact from defective provirus via two strategically placed amplicons in HIV psi and RRE regions as well as a hypermutation discrimination probe, and (2) the Copy Reference/Shearing reaction, which quantifies DNA shearing and input diploid cell equivalents using the human *RPP30* gene.[85] All ddPCR reactions were assembled via automated liquid handles to maximize reproducibility and analyzed using the BioRad QX200 AutoDG Digital Droplet PCR system (BioRad). Up to 700 ng of genomic DNA were analyzed per reaction, and final input DNA concentrations were dependent upon recovered DNA concentrations. Samples were batch processed and analyzed, including negative controls from uninfected donors and J-Lat full-length clone 6.3 (E. Verdin, Gladstone Institutes and UCSF, San Francisco, CA, USA) cells as positive controls. Across >500 IPDA measurements, we interrogated a median of 4.8×10^5 CD4+ T cell genomes per assay and observed a median DNA shearing index (DSI) of 0.40.

Statistical Methods

We developed a novel semiparametric biphasic decay model to estimate the HIV DNA reservoir size over time in $\log_{10}$ copies per 10^6 CD4+ T cells as

$$\log_{10}(I_{it}) \sim f_1(T_{it}; \tau, \beta_1, \beta_2) + E_i \cdot f_1(T_{it}; \tau, \beta_3, \beta_4) + f_2(C_i) + f_3(V_i) + \mu_i, \#(1)$$

where in I_{it} represents either the HIV intact or defective DNA reservoir size, of the i-th participant at t-th visit. The number of weeks since ART initiation is denoted T_{it}. The model additionally accounts for baseline clinical information defined as the initial CD4+ T cell count, C_i, pre-ART viral load, V_i, and the estimated time between HIV infection and ART initiation, E_i. The delay in ART initiation was centered to have a mean of zero prior to analysis; this offset was approximately 60 days in our cohort. Participant-level random effects, μ_i, are also included. Building on existing models,[3,57] we parameterized the decay as a continuous, linear spline with a single knot at τ: $f_1(T_{it}; \tau, \beta_1, \beta_2) = \beta_1 \cdot \min\{T_{it}, \tau\} + \beta_2 \cdot \max\{T_{it} - \tau, 0\}$. Under this parameterization, β_1 and β_2 represent the decay rate before and after τ, respectively. For triphasic models, the decay was modeled as a continuous, linear spline with knots at τ_1 and τ_2. For monophasic models, the decay was modeled as a linear function of time. The same spline parameterization and inflection point(s) were used to model the time on ART and interaction between time on ART and delay in ART initiation; different slopes were estimated for these two terms. Cubic splines were used for both $f_2(C_i)$ and $f_3(V_i)$. After fixing the inflection point(s), model estimation was performed using the mgcv (v1.9-1) package in R (4.3.1). A two-sided Welch's t-test was used to compare decay rate estimates across models.

Regardless of the HIV measure (intact DNA, defective DNA, or plasma RNA), the inflection point, τ, was estimated by minimizing the model's mean absolute prediction error. Candidate τ values were tested iteratively (from 0 weeks to 24 weeks) and the mean absolute errors (MAEs) were estimated using leave-one-out cross-validation:

$$MAE(\tau) = \sum_{i,t} \left| \log_{10}(I_{it}) - \log_{10}\left(\hat{I}_{it}^{(-i)}\right) \right|, \#(2)$$

where $\hat{I}_{it}^{(-i)}$ reflected the predicted HIV DNA counts for participant i at time t using the model fit for each participant (excluding participant i). Inflection points for the triphasic model were estimated similarly. We then compared the fit of various models using Akaike information criteria (AIC).

To facilitate the interpretability of our results and to allow direct comparison with prior reports,[3,52,58] we estimated decay half-lives, and their confidence intervals for each phase of decay, using the multivariate delta method.[86] For example, the half-life in the first decay phase, from model (1), was calculated as

$$t_{1/2}(E_i) = -\frac{0.25\log_{10}(2)}{\beta_1 + \beta_2 E_i} = -\frac{0.25\log_{10}(2)}{\beta_1} + \frac{0.25\log_{10}(2)\,\beta_2 E_i}{\beta_1^2} + O\left(E_i^2\right), \#(3)$$

where the second equality reflected the degree-one Taylor series about $E_i = 0$. We centered E_i prior to model estimation to justify the degree-one Taylor series approximation of half-life. Thus, we estimated the baseline $t_{1/2}$ as $g_1(\beta_1, \beta_3) = -0.25\log_{10}(2)/\beta_1$ and the adjusted $t_{1/2}$ (for each week delay in ART initiation) as $g_2(\beta_1, \beta_2) = 0.25\log_{10}(2)\,\beta_2/\beta_1^2$. Finally, we included our estimated model parameters into the delta method to obtain half-life estimates:

$$\sqrt{n}\left(\begin{bmatrix} g_1(\widehat{\beta_1}, \widehat{\beta_2}) \\ g_2(\widehat{\beta_1}, \widehat{\beta_2}) \end{bmatrix} - \begin{bmatrix} g_1(\beta_1, \beta_2) \\ g_2(\beta_1, \beta_2) \end{bmatrix}\right) \xrightarrow{d} N\left(\begin{pmatrix} 0 \\ 0 \end{pmatrix}, J\,\Sigma\,J^T\right) \#(4)$$

$$J = 0.25\log_{10}(2)\begin{bmatrix} \frac{1}{\beta_1^2} & 0 \\ -2\frac{\beta_2}{\beta_1^2} & \frac{1}{\beta_1^2} \end{bmatrix}, \#(5)$$

where Σ reflected the covariance between β_1 and β_2, and J was the Jacobian matrix of $g(\beta_1, \beta_2)$. For further interpretability, we calculated the percent decay/week (prior to τ) using the transformation $h(\beta_1) = -100\,(2^{\beta_1} - 1)$. Similar calculations were performed for the second decay phase using β_3 and β_4 instead of β_1 and β_2.

We performed further validation of our proposed HIV DNA (intact, defective) and HIV RNA (plasma) decay models against known clinical factors associated with HIV reservoir size.[23,24,34,42,43] Focusing on the clinical covariates of (i) initial CD4+ T cell count, (ii) pre-ART viral load, and (iii) timing of ART initiation (days from HIV infection to ART start date), we performed bootstrapping predictions by resampling and generating 300 new participants. The final HIV decay models (intact DNA, defective DNA, plasma RNA) were used to predict decay patterns for each resampled (bootstrapped) participant. For data visualization, we partitioned the resampled data into tertiles to demonstrate average predicted decay patterns by tertiles of each clinical predictor.

Table 1. UCSF Treat Acute HIV Study Population. Medians (with interquartile ranges) or frequencies (with percentages) are shown.

	N = 67
Timing of ART initiation (days from date of detected HIV infection to ART start date)	31.0 (22.0 – 88.5)
Initial CD4+ T-cell count (cells/mm^3)	505 (350 – 670)
Pre-ART plasma HIV RNA (log_{10} copies)	4.85 (3.69 – 5.65)
Age	30.0 (25.5 – 38.0)
Gender (self-reported)	
Male	65 (97.0%)
Cisgender Female	1 (1.50%)
Transgender Female	1 (1.50%)
Race/ethnicity (self-reported)	
White	22 (32.8%)
Latinx	20 (29.9%)
Asian	14 (20.9%)
Black	10 (14.9%)
Other	1 (1.5%)
Prior pre-exposure prophylaxis (PrEP)	29 (43.3%)
HIV acquisition/PrEP overlap <10 days	15 (22.4%)
PrEP initiated but already acquired HIV	8 (11.9%)
HIV acquired on PrEP [a]	6 (9.0%)
Referral HIV testing sites	
San Francisco Department Public Health (%)	28 (41.8%)
Community-Based Organization (%)	29 (43.2%)
Private Health Clinics (%)	10 (14.9%)
Unstably housed	2 (3.0%)

[a] For participants with HIV acquired on PrEP: median baseline plasma log_{10}HIV RNA was 2.2 copies/mL.

Fig. 1: The distribution of study participants in the UCSF Treat Acute HIV cohort. A total of 67 participants met inclusion criteria for acute HIV, defined as <100 days since the estimated date of detected HIV infection (EDDI) using the Infection Dating Tool (https://tools.incidence-estimation.org/idt/); these estimates were then used to estimate acute HIV Fiebig stages (a).[47,48] The majority of the cohort was of non-White self-reported race/ethnicity, consistent with national trends for people incident acute HIV (b).[49]

a.

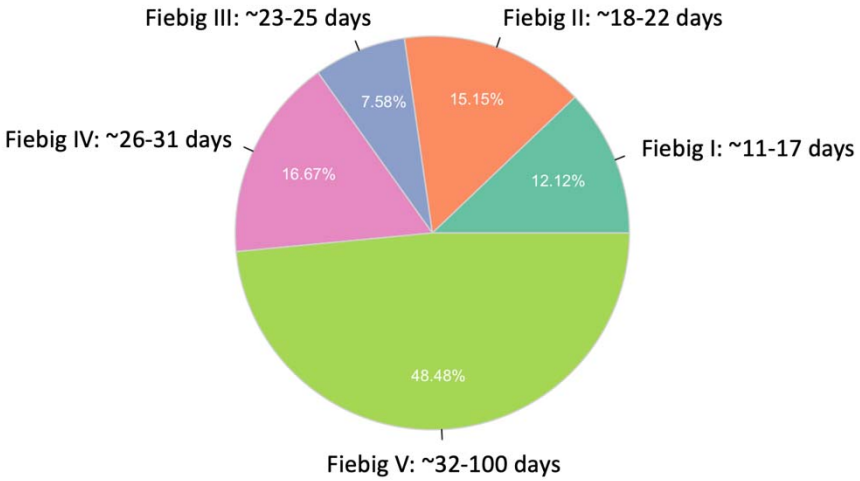

b.

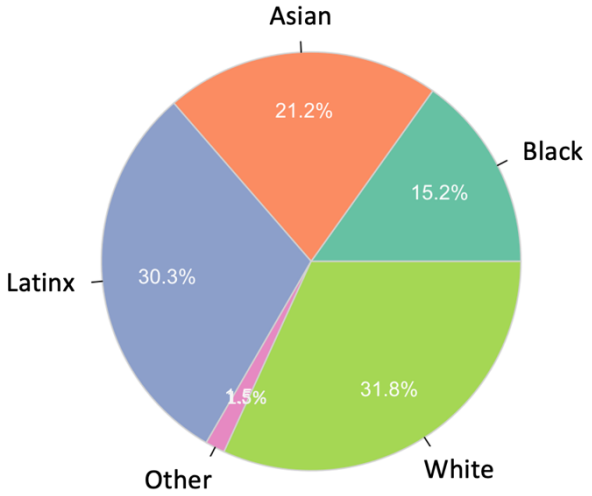

Fig. 2: Semiparametric monophasic, biphasic, and triphasic generalized additive models of HIV reservoir decay during weeks 0-24. We performed bootstrapping to estimate the Akaike information criteria (AIC) value and 95% confidence intervals and compared monophasic, biphasic, and triphasic models for both HIV intact (left panels) and defective (right panels) DNA assays (a). Using the triphasic models for HIV intact (left panel) and defective (right panel) DNA, we then determined the optimal inflection point(s), τ, by minimizing the predicted mean absolute error (MAE; top panels) using leave-one-out cross-validation or the predicted mean squared error (MSE; bottom panels) (b). Red dots denote the optimal inflection point(s), τ, for each model and prediction loss metric. For HIV intact DNA, the first (x-axis) and second (y-axis) inflection points were relatively similar, suggesting that a single inflection point – i.e., a biphasic model – adequately described the data. For HIV defective DNA, the first inflection point (x-axis) was close to zero, this again suggested that a biphasic model reasonably described the data.

a.

HIV Reservoir	Monophasic (95% CI)	Biphasic (95% CI)	Triphasic (95% CI)
Intact DNA	886 (722, 1023)	797 (595, 968)	796 (597, 965)
Defective DNA	1426 (1344, 1504)	1268 (1183, 1343)	1272 (1188, 1348)

b.

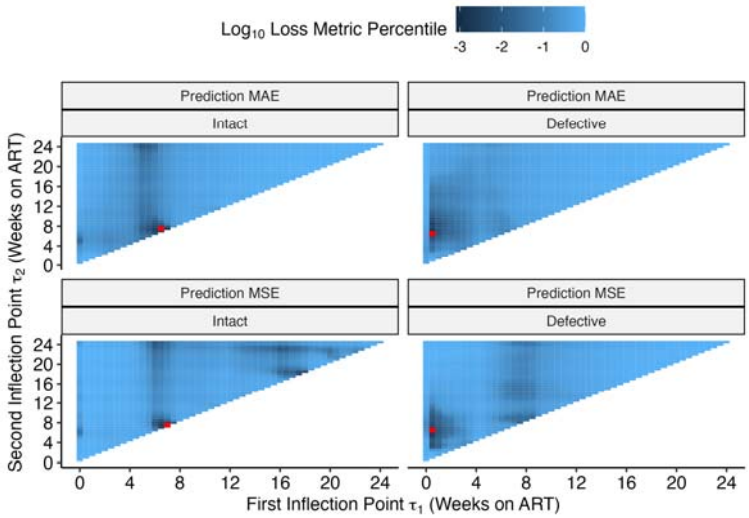

Fig. 3 Determination of optimal inflection points for HIV intact and defective DNA biphasic decay models. Using the biphasic models for HIV intact (left panel) and defective (right panel) DNA, we then determined the optimal inflection point(s), τ, by minimizing the predicted mean absolute error (MAE; top panels) using leave-one-out cross-validation or the predicted mean squared error (MSE; bottom panels) (b). An inflection point of τ = 5 weeks (vertical dashed line) best fit decay patterns for both HIV intact (left panels) and defective (right panels) DNA. Red dots denote the best τ for each model and prediction error metric.

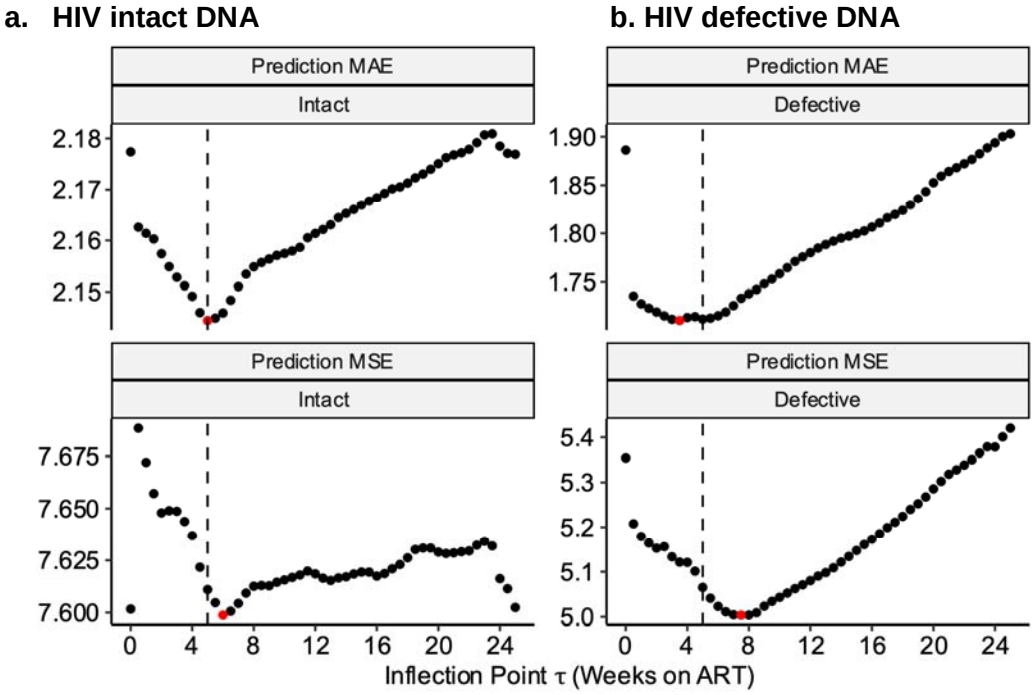

Fig. 4 Predicted decay patterns of HIV intact and defective DNA during acute treated HIV from weeks 0-24. Decay patterns for observed (thin grey lines) HIV intact and total defective (a), as well as 3' and 5' defective (b) DNA closely fit with average model predictions (thick black lines). Sampling timepoints are labeled on the x-axis (including a week 2 study visit during which confirmatory HIV test results were disclosed). We estimated average predicted participant decay rates by taking the mean of (estimated time between HIV infection and ART initiation), (initial CD4+ T cell count), and (log_{10} pre-ART plasma viral load) across participants from final models.

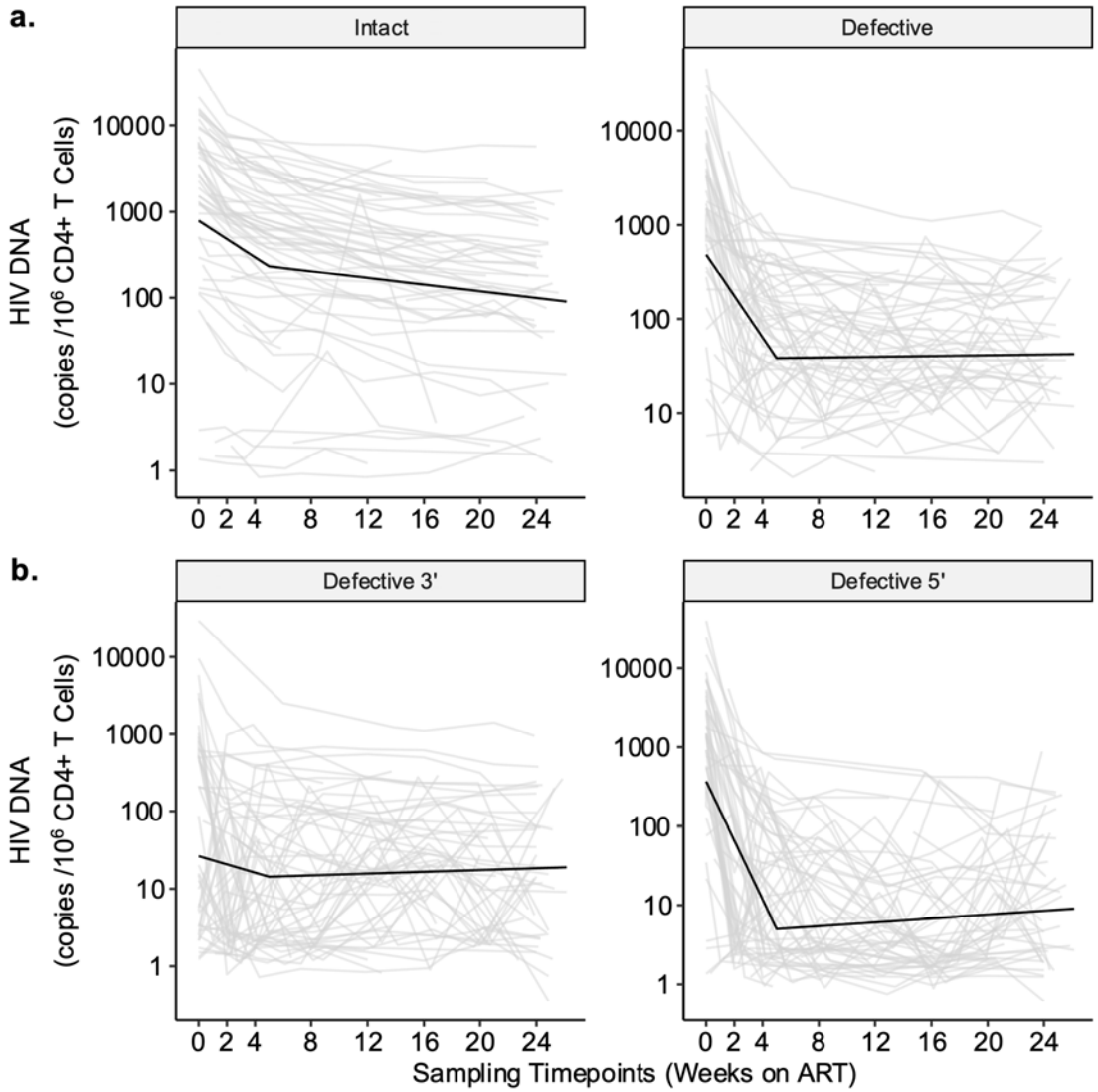

Fig. 5 HIV intact and defective DNA decay patterns were associated with known clinical factors associated with HIV reservoir size. The observed HIV DNA data are shown as thin grey lines for each participant, while the decay pattern for the model-predicted average participant is shown as the thick black lines. Biphasic decay patterns for HIV intact (left panel) and combined defective (3' plus 5', right panel) were faster among participants initiating ART earlier (<30 days vs. 30-100 days) (a), with higher initial CD4+ T cell counts (shown by tertiles) (b), and lower pre-ART viral load (shown by tertiles) (c).

a.

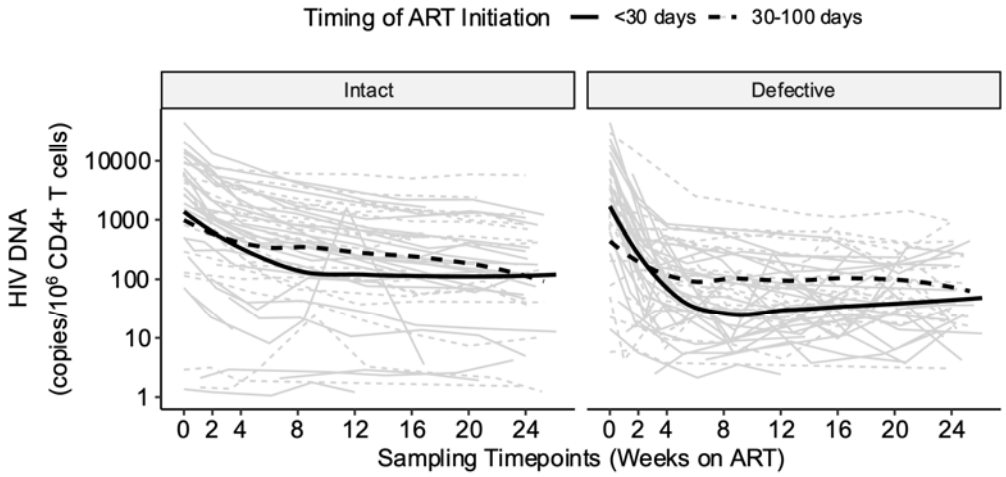

b.

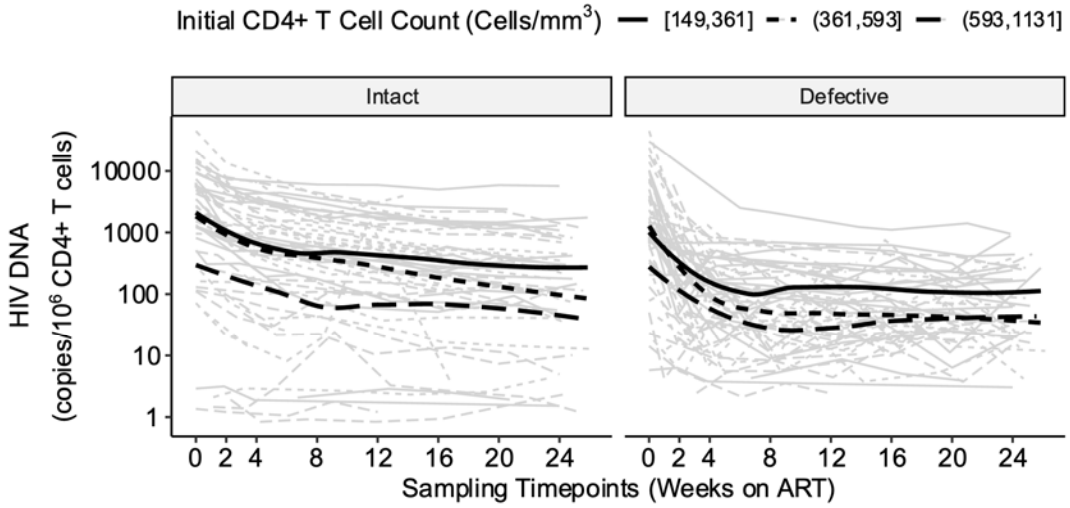

c.

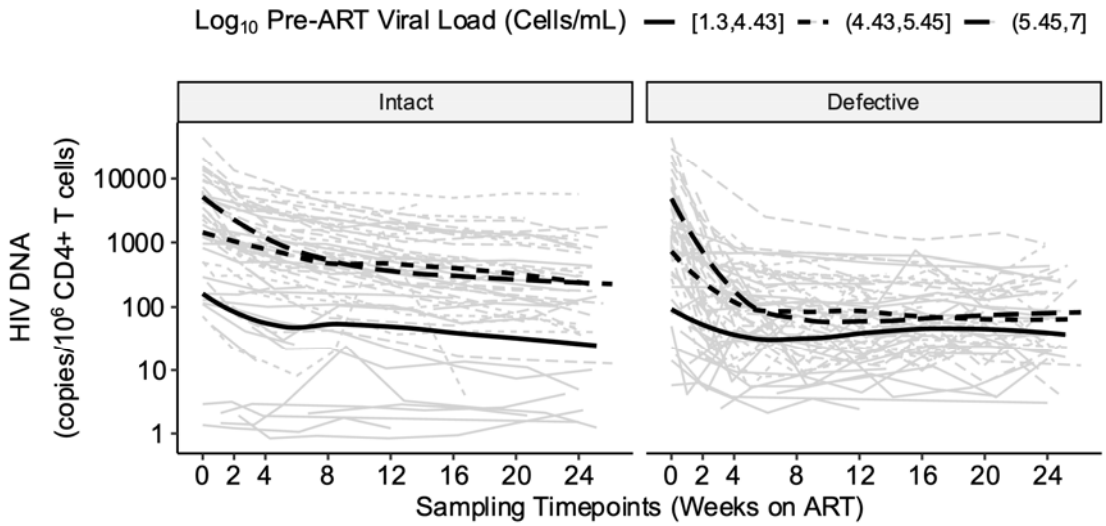

Fig. 6 Predicted HIV intact and defective DNA decay rates, by tertiles of clinical factors associated with HIV reservoir size. We performed bootstrapping to estimate the average predicted decay rates of HIV intact (left panels) and defective (right panels) DNA, stratified by tertiles of known clinical factors associated with HIV reservoir size: timing of ART initiation (a), initial CD4+ T cell count (b), and pre-ART viral load (c).

a.

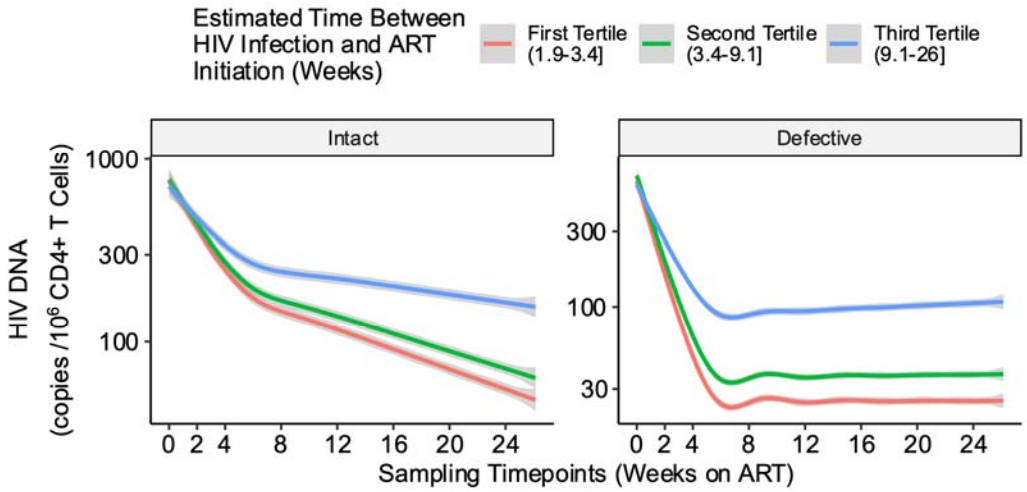

b.

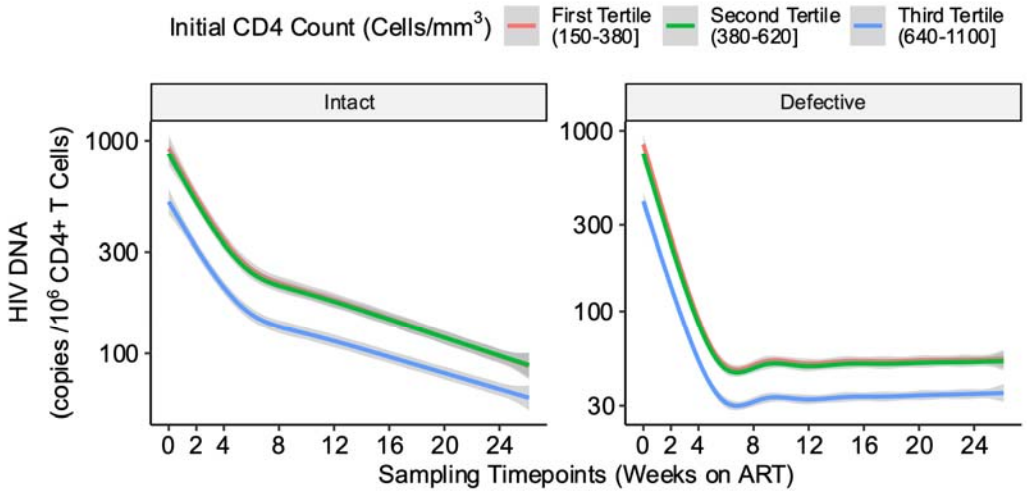

12 **c.**

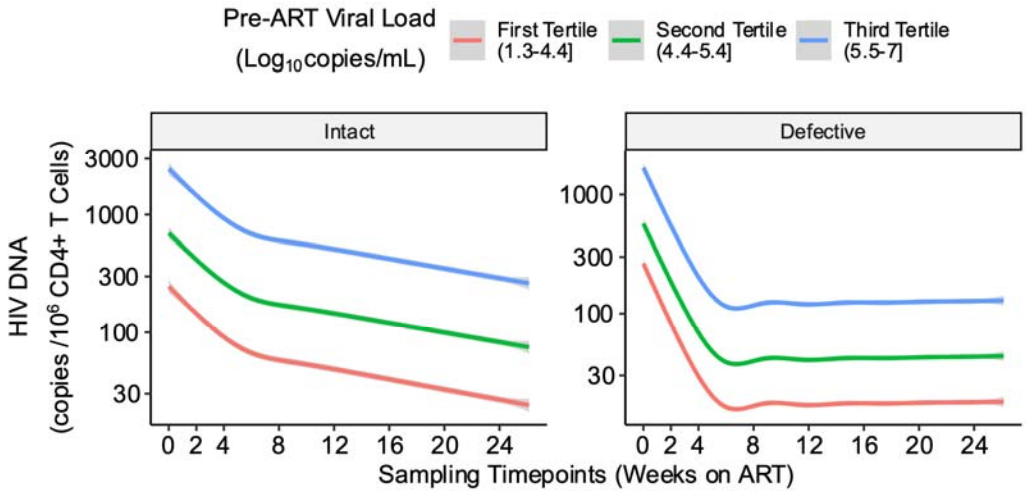

13

14

REFERENCES

1 Chun, T. W. *et al.* Rebound of plasma viremia following cessation of antiretroviral therapy despite profoundly low levels of HIV reservoir: implications for eradication. *AIDS* **24**, 2803-2808 (2010). https://doi.org:10.1097/QAD.0b013e328340a239

2 Hocqueloux, L. *et al.* Long-term immunovirologic control following antiretroviral therapy interruption in patients treated at the time of primary HIV-1 infection. *AIDS* **24**, 1598-1601 (2010). https://doi.org:10.1097/qad.0b013e32833b61ba

3 White, J. A. *et al.* Complex decay dynamics of HIV virions, intact and defective proviruses, and 2LTR circles following initiation of antiretroviral therapy. *Proc Natl Acad Sci U S A* **119** (2022). https://doi.org:10.1073/pnas.2120326119

4 Perelson, A. S. *et al.* Decay characteristics of HIV-1-infected compartments during combination therapy. *Nature* **387**, 188-191 (1997). https://doi.org:10.1038/387188a0

5 Kwon, K. J. & Siliciano, R. F. HIV persistence: clonal expansion of cells in the latent reservoir. *J Clin Invest* **127**, 2536-2538 (2017). https://doi.org:10.1172/JCI95329

6 Finzi, D. & Siliciano, R. F. Viral dynamics in HIV-1 infection. *Cell* **93**, 665-671 (1998). https://doi.org:10.1016/s0092-8674(00)81427-0

7 Chomont, N. *et al.* HIV reservoir size and persistence are driven by T cell survival and homeostatic proliferation. *Nature medicine* **15**, 893-900 (2009). https://doi.org:10.1038/nm.1972

8 Yukl, S. A. *et al.* Differences in HIV burden and immune activation within the gut of HIV-positive patients receiving suppressive antiretroviral therapy. *The Journal of infectious diseases* **202**, 1553-1561 (2010). https://doi.org:10.1086/656722

9 Archin, N. M. *et al.* Administration of vorinostat disrupts HIV-1 latency in patients on antiretroviral therapy. *Nature* **487**, 482-485 (2012). https://doi.org:10.1038/nature11286

10 Elliott, J. H. *et al.* Short-term administration of disulfiram for reversal of latent HIV infection: a phase 2 dose-escalation study. *Lancet HIV* **2**, e520-529 (2015). https://doi.org:10.1016/S2352-3018(15)00226-X

11 Rasmussen, T. A. *et al.* Panobinostat, a histone deacetylase inhibitor, for latent-virus reactivation in HIV-infected patients on suppressive antiretroviral therapy: a phase 1/2, single group, clinical trial. *Lancet HIV* **1**, e13-21 (2014). https://doi.org:10.1016/S2352-3018(14)70014-1

12 Elliott, J. H. *et al.* Activation of HIV transcription with short-course vorinostat in HIV-infected patients on suppressive antiretroviral therapy. *PLoS pathogens* **10**, e1004473 (2014). https://doi.org:10.1371/journal.ppat.1004473

13 Gay, C. L. *et al.* Assessing the impact of AGS-004, a dendritic cell-based immunotherapy, and vorinostat on persistent HIV-1 Infection. *Sci Rep* **10**, 5134 (2020). https://doi.org:10.1038/s41598-020-61878-3

14 Fidler, S. *et al.* Antiretroviral therapy alone versus antiretroviral therapy with a kick and kill approach, on measures of the HIV reservoir in participants with recent HIV infection (the RIVER trial): a phase 2, randomised trial. *Lancet* **395**, 888-898 (2020). https://doi.org:10.1016/S0140-6736(19)32990-3

15 Gutierrez, C. *et al.* Bryostatin-1 for latent virus reactivation in HIV-infected patients on antiretroviral therapy. *AIDS* **30**, 1385-1392 (2016). https://doi.org:10.1097/QAD.0000000000001064

16 Vibholm, L. *et al.* Short-Course Toll-Like Receptor 9 Agonist Treatment Impacts Innate Immunity and Plasma Viremia in Individuals With Human Immunodeficiency Virus Infection. *Clin Infect Dis* **64**, 1686-1695 (2017). https://doi.org:10.1093/cid/cix201

17 Riddler, S. A. *et al.* Vesatolimod, a Toll-like Receptor 7 Agonist, Induces Immune Activation in Virally Suppressed Adults Living With Human Immunodeficiency Virus-1. *Clin Infect Dis* **72**, e815-e824 (2021). https://doi.org:10.1093/cid/ciaa1534

18 Elliott, J. H. *et al.* Short-term administration of disulfiram for reversal of latent HIV infection: a phase 2 dose-escalation study. *Lancet HIV* **2**, e520-529 (2015). https://doi.org:10.1016/S2352-3018(15)00226-X

19 Bar, K. J. *et al.* Effect of HIV Antibody VRC01 on Viral Rebound after Treatment Interruption. *N Engl J Med* **375**, 2037-2050 (2016). https://doi.org:10.1056/NEJMoa1608243

20 Gunst, J. D. *et al.* Early intervention with 3BNC117 and romidepsin at antiretroviral treatment initiation in people with HIV-1: a phase 1b/2a, randomized trial. *Nat Med* **28**, 2424-2435 (2022). https://doi.org:10.1038/s41591-022-02023-7

21 Gunst, J. D. *et al.* in *Conference on Retroviruses and Opportunistic Infections.*

22 Namazi, G. *et al.* The Control of HIV After Antiretroviral Medication Pause (CHAMP) Study: Posttreatment Controllers Identified From 14 Clinical Studies. *J Infect Dis* **218**, 1954-1963 (2018). https://doi.org:10.1093/infdis/jiy479

23 Archin, N. M. *et al.* Immediate antiviral therapy appears to restrict resting CD4+ cell HIV-1 infection without accelerating the decay of latent infection. *Proc Natl Acad Sci U S A* **109**, 9523-9528 (2012). https://doi.org:10.1073/pnas.1120248109

24 Buzon, M. J. *et al.* Long-term antiretroviral treatment initiated at primary HIV-1 infection affects the size, composition, and decay kinetics of the reservoir of HIV-1-infected CD4 T cells. *J Virol* **88**, 10056-10065 (2014). https://doi.org:10.1128/JVI.01046-14

25 Chun, T. W. *et al.* Early establishment of a pool of latently infected, resting CD4(+) T cells during primary HIV-1 infection. *Proc Natl Acad Sci U S A* **95**, 8869-8873 (1998). https://doi.org:10.1073/pnas.95.15.8869

26 Strain, M. C. *et al.* Effect of treatment, during primary infection, on establishment and clearance of cellular reservoirs of HIV-1. *J Infect Dis* **191**, 1410-1418 (2005). https://doi.org:10.1086/428777

27 Hocqueloux, L., Saez-Cirion, A. & Rouzioux, C. Immunovirologic control 24 months after interruption of antiretroviral therapy initiated close to HIV seroconversion. *JAMA Intern Med* **173**, 475-476 (2013). https://doi.org:10.1001/jamainternmed.2013.2176

28 Ananworanich, J. *et al.* Virological and immunological characteristics of HIV-infected individuals at the earliest stage of infection. *J Virus Erad* **2**, 43-48 (2016).

29 Ananworanich, J. *et al.* Impact of multi-targeted antiretroviral treatment on gut T cell depletion and HIV reservoir seeding during acute HIV infection. *PLoS One* **7**, e33948 (2012). https://doi.org:10.1371/journal.pone.0033948

30 Deleage, C. *et al.* Impact of early cART in the gut during acute HIV infection. *JCI Insight* **1** (2016). https://doi.org:10.1172/jci.insight.87065

31 Takata, H. *et al.* Long-term antiretroviral therapy initiated in acute HIV infection prevents residual dysfunction of HIV-specific CD8(+) T cells. *EBioMedicine* **84**, 104253 (2022). https://doi.org:10.1016/j.ebiom.2022.104253

32 Oxenius, A. *et al.* Early highly active antiretroviral therapy for acute HIV-1 infection preserves immune function of CD8+ and CD4+ T lymphocytes. *Proc Natl Acad Sci U S A* **97**, 3382-3387 (2000). https://doi.org:10.1073/pnas.97.7.3382

33 Streeck, H. *et al.* Immunological and virological impact of highly active antiretroviral therapy initiated during acute HIV-1 infection. *J Infect Dis* **194**, 734-739 (2006). https://doi.org:10.1086/503811

34 Peluso, M. J. *et al.* Differential decay of intact and defective proviral DNA in HIV-1-infected individuals on suppressive antiretroviral therapy. *JCI Insight* **5** (2020). https://doi.org:10.1172/jci.insight.132997

35 Gandhi, R. T. *et al.* Selective Decay of Intact HIV-1 Proviral DNA on Antiretroviral Therapy. *J Infect Dis* **223**, 225-233 (2021). https://doi.org:10.1093/infdis/jiaa532

36 Gandhi, R. T. *et al.* Varied Patterns of Decay of Intact Human Immunodeficiency Virus Type 1 Proviruses Over 2 Decades of Antiretroviral Therapy. *J Infect Dis* **227**, 1376-1380 (2023). https://doi.org:10.1093/infdis/jiad039

37 Antar, A. A. *et al.* Longitudinal study reveals HIV-1-infected CD4+ T cell dynamics during long-term antiretroviral therapy. *J Clin Invest* **130**, 3543-3559 (2020). https://doi.org:10.1172/JCI135953

38 Leyre, L. *et al.* Abundant HIV-infected cells in blood and tissues are rapidly cleared upon ART initiation during acute HIV infection. *Sci Transl Med* **12** (2020). https://doi.org:10.1126/scitranslmed.aav3491

39 Massanella, M. *et al.* Long-term effects of early antiretroviral initiation on HIV reservoir markers: a longitudinal analysis of the MERLIN clinical study. *Lancet Microbe* **2**, e198-e209 (2021). https://doi.org:10.1016/S2666-5247(21)00010-0

40 De Clercq, J. *et al.* Longitudinal patterns of inflammatory mediators after acute HIV infection correlate to intact and total reservoir. *Front Immunol* **14**, 1337316 (2023). https://doi.org:10.3389/fimmu.2023.1337316

41 Shi, L. *et al.* in *International AIDS Society Conference on HIV Science.*

42 Ananworanich, J. *et al.* HIV DNA Set Point is Rapidly Established in Acute HIV Infection and Dramatically Reduced by Early ART. *EBioMedicine* **11**, 68-72 (2016). https://doi.org:10.1016/j.ebiom.2016.07.024

43 Crowell, T. A. *et al.* Virologic failure is uncommon after treatment initiation during acute HIV infection. *AIDS* **30**, 1943-1950 (2016). https://doi.org:10.1097/QAD.0000000000001148

44 Lee SA, H. T., Gandhi M, Coffey S, Harting H, Hoh R, Peluso MJ, Siegel D, Crouch P, Scott H, Cohen SD, Sachdev D, Bacon O, Busch M, Pilcher C, Buchbinder S, Havlir DV, Deeks SG. in *International AIDS Society Conference.*

45 Grebe, E. *et al.* Interpreting HIV diagnostic histories into infection time estimates: analytical framework and online tool. *BMC Infect Dis* **19**, 894 (2019). https://doi.org:10.1186/s12879-019-4543-9

46 Facente, S. N. *et al.* Estimated dates of detectable infection (EDDIs) as an improvement upon Fiebig staging for HIV infection dating. *Epidemiol Infect* **148**, e53 (2020). https://doi.org:10.1017/S0950268820000503

47 Fiebig, E. W. *et al.* Dynamics of HIV viremia and antibody seroconversion in plasma donors: implications for diagnosis and staging of primary HIV infection. *AIDS* **17**, 1871-1879 (2003). https://doi.org:10.1097/01.aids.0000076308.76477.b8

48 Keele, B. F. *et al.* Identification and characterization of transmitted and early founder virus envelopes in primary HIV-1 infection. *Proc Natl Acad Sci U S A* **105**, 7552-7557 (2008). https://doi.org:10.1073/pnas.0802203105

49 Prevention., C. f. D. C. a. HIV Surveillance Report. http://www.cdc.gov/hiv/library/reports/hiv-surveillance.html. Published May 2022. Accessed Nov 2, 2023., (2020).

50 Buchbinder, S. P. & Havlir, D. V. Getting to Zero San Francisco: A Collective Impact Approach. *J Acquir Immune Defic Syndr* **82 Suppl 3**, S176-S182 (2019). https://doi.org:10.1097/QAI.0000000000002200

51 Cohen, S. E. *et al.* Acquisition of tenofovir-susceptible, emtricitabine-resistant HIV despite high adherence to daily pre-exposure prophylaxis: a case report. *Lancet HIV* (2018). https://doi.org:10.1016/S2352-3018(18)30288-1

52 Andrade, A. *et al.* Three distinct phases of HIV-1 RNA decay in treatment-naive patients receiving raltegravir-based antiretroviral therapy: ACTG A5248. *J Infect Dis* **208**, 884-891 (2013). https://doi.org:10.1093/infdis/jit272

53 Raffi, F. *et al.* Once-daily dolutegravir versus twice-daily raltegravir in antiretroviral-naive adults with HIV-1 infection (SPRING-2 study): 96 week results from a randomised, double-blind, non-inferiority trial. *Lancet Infect Dis* **13**, 927-935 (2013). https://doi.org:10.1016/S1473-3099(13)70257-3

54 Powderly, W. G. Integrase inhibitors in the treatment of HIV-1 infection. *J Antimicrob Chemother* **65**, 2485-2488 (2010). https://doi.org:10.1093/jac/dkq350

55 Reeves, D. B. *et al.* Impact of misclassified defective proviruses on HIV reservoir measurements. *Nat Commun* **14**, 4186 (2023). https://doi.org:10.1038/s41467-023-39837-z

56 Reeves, D. B. *et al.* A majority of HIV persistence during antiretroviral therapy is due to infected cell proliferation. *Nat Commun* **9**, 4811 (2018). https://doi.org:10.1038/s41467-018-06843-5

57 McMyn, N. F. *et al.* The latent reservoir of inducible, infectious HIV-1 does not decrease despite decades of antiretroviral therapy. *J Clin Invest* **133** (2023). https://doi.org:10.1172/JCI171554

58 Massanella, M. *et al.* Long-term effects of early antiretroviral initiation on HIV reservoir markers: a longitudinal analysis of the MERLIN clinical study. *Lancet Microbe* **2**, e198-e209 (2021). https://doi.org:10.1016/s2666-5247(21)00010-0

59 Fromentin, R. *et al.* CD4+ T Cells Expressing PD-1, TIGIT and LAG-3 Contribute to HIV Persistence during ART. *PLoS Pathog* **12**, e1005761 (2016). https://doi.org:10.1371/journal.ppat.1005761

60 Fromentin, R. *et al.* PD-1 blockade potentiates HIV latency reversal ex vivo in CD4(+) T cells from ART-suppressed individuals. *Nat Commun* **10**, 814 (2019). https://doi.org:10.1038/s41467-019-08798-7

61 Murray, J. M., Kelleher, A. D. & Cooper, D. A. Timing of the components of the HIV life cycle in productively infected CD4+ T cells in a population of HIV-infected individuals. *J Virol* **85**, 10798-10805 (2011). https://doi.org:10.1128/JVI.05095-11

62 Gilmore, J. B., Kelleher, A. D., Cooper, D. A. & Murray, J. M. Explaining the determinants of first phase HIV decay dynamics through the effects of stage-dependent drug action. *PLoS Comput Biol* **9**, e1002971 (2013). https://doi.org:10.1371/journal.pcbi.1002971

63 Perelson, A. S., Neumann, A. U., Markowitz, M., Leonard, J. M. & Ho, D. D. HIV-1 dynamics in vivo: virion clearance rate, infected cell life-span, and viral generation time. *Science* **271**, 1582-1586 (1996). https://doi.org:10.1126/science.271.5255.1582

64 Markowitz, M. *et al.* A novel antiviral intervention results in more accurate assessment of human immunodeficiency virus type 1 replication dynamics and T-cell decay in vivo. *J Virol* **77**, 5037-5038 (2003). https://doi.org:10.1128/jvi.77.8.5037-5038.2003

65 Shan, L. *et al.* Transcriptional Reprogramming during Effector-to-Memory Transition Renders CD4(+) T Cells Permissive for Latent HIV-1 Infection. *Immunity* **47**, 766-775 e763 (2017). https://doi.org:10.1016/j.immuni.2017.09.014

66 De Boer, R. J., Homann, D. & Perelson, A. S. Different dynamics of CD4+ and CD8+ T cell responses during and after acute lymphocytic choriomeningitis virus infection. *J Immunol* **171**, 3928-3935 (2003). https://doi.org:10.4049/jimmunol.171.8.3928

67 Zhan, Y., Carrington, E. M., Zhang, Y., Heinzel, S. & Lew, A. M. Life and Death of Activated T Cells: How Are They Different from Naive T Cells? *Front Immunol* **8**, 1809 (2017). https://doi.org:10.3389/fimmu.2017.01809

68 Siliciano, J. D. *et al.* Long-term follow-up studies confirm the stability of the latent reservoir for HIV-1 in resting CD4+ T cells. *Nat Med* **9**, 727-728 (2003). https://doi.org:10.1038/nm880

69 Crooks, A. M. *et al.* Precise Quantitation of the Latent HIV-1 Reservoir: Implications for Eradication Strategies. *J Infect Dis* **212**, 1361-1365 (2015). https://doi.org:10.1093/infdis/jiv218

70 Vandergeeten, C. *et al.* Cross-clade ultrasensitive PCR-based assays to measure HIV persistence in large-cohort studies. *J Virol* **88**, 12385-12396 (2014). https://doi.org:10.1128/JVI.00609-14

71 Finzi, D. *et al.* Identification of a reservoir for HIV-1 in patients on highly active antiretroviral therapy. *Science* **278**, 1295-1300 (1997). https://doi.org:10.1126/science.278.5341.1295

72 Procopio, F. A. *et al.* A Novel Assay to Measure the Magnitude of the Inducible Viral Reservoir in HIV-infected Individuals. *EBioMedicine* **2**, 872-881 (2015). https://doi.org:10.1016/j.ebiom.2015.06.019

73 Ho, Y. C. *et al.* Replication-competent noninduced proviruses in the latent reservoir increase barrier to HIV-1 cure. *Cell* **155**, 540-551 (2013). https://doi.org:10.1016/j.cell.2013.09.020

74 Eriksson, S. *et al.* Comparative analysis of measures of viral reservoirs in HIV-1 eradication studies. *PLoS pathogens* **9**, e1003174 (2013). https://doi.org:10.1371/journal.ppat.1003174

75 Pollack, R. A. *et al.* Defective HIV-1 Proviruses Are Expressed and Can Be Recognized by Cytotoxic T Lymphocytes, which Shape the Proviral Landscape. *Cell Host Microbe* **21**, 494-506 e494 (2017). https://doi.org:10.1016/j.chom.2017.03.008

76 Simon, V. & Ho, D. D. HIV-1 dynamics in vivo: implications for therapy. *Nat Rev Microbiol* **1**, 181-190 (2003). https://doi.org:10.1038/nrmicro772

77 Siliciano, J. D. *et al.* Long-term follow-up studies confirm the stability of the latent reservoir for HIV-1 in resting CD4+ T cells. *Nature medicine* **9**, 727-728 (2003). https://doi.org:10.1038/nm880

78 Pinzone, M. R. *et al.* Longitudinal HIV sequencing reveals reservoir expression leading to decay which is obscured by clonal expansion. *Nat Commun* **10**, 728 (2019). https://doi.org:10.1038/s41467-019-08431-7

79 Gondim, M. V. P. *et al.* Heightened resistance to host type 1 interferons characterizes HIV-1 at transmission and after antiretroviral therapy interruption. *Sci Transl Med* **13** (2021). https://doi.org:10.1126/scitranslmed.abd8179

80 Kinloch, N. N. *et al.* HIV-1 diversity considerations in the application of the Intact Proviral DNA Assay (IPDA). *Nat Commun* **12**, 165 (2021). https://doi.org:10.1038/s41467-020-20442-3

81 Whitney, J. B. *et al.* Rapid seeding of the viral reservoir prior to SIV viraemia in rhesus monkeys. *Nature* **512**, 74-77 (2014). https://doi.org:10.1038/nature13594

82 Kumar, M. R. *et al.* Biphasic decay of intact SHIV genomes following initiation of antiretroviral therapy complicates analysis of interventions targeting the reservoir. *Proc Natl Acad Sci U S A* **120**, e2313209120 (2023). https://doi.org:10.1073/pnas.2313209120

83 Martin, A. R. *et al.* Similar Frequency and Inducibility of Intact Human Immunodeficiency Virus-1 Proviruses in Blood and Lymph Nodes. *J Infect Dis* **224**, 258-268 (2021). https://doi.org:10.1093/infdis/jiaa736

84 Simonetti, F. R. *et al.* Intact proviral DNA assay analysis of large cohorts of people with HIV provides a benchmark for the frequency and composition of persistent proviral DNA. *Proc Natl Acad Sci U S A* **117**, 18692-18700 (2020). https://doi.org:10.1073/pnas.2006816117

85 Bruner, K. M. *et al.* A quantitative approach for measuring the reservoir of latent HIV-1 proviruses. *Nature* **566**, 120-125 (2019). https://doi.org:10.1038/s41586-019-0898-8

86 Lehmann, E. L. & Casella, G. *Theory of point estimation*. Second edition. edn, (Springer, 1998).

FIGURE LEGENDS

Table 1. UCSF Treat Acute HIV Study Population. Medians (with interquartile ranges) or frequencies (with percentages) are shown.

Fig. 1: The distribution of study participants in the UCSF Treat Acute HIV cohort. A total of 67 participants met inclusion criteria for acute HIV, defined as <100 days since the estimated date of detected HIV infection (EDDI) using the Infection Dating Tool (https://tools.incidence-estimation.org/idt/); these estimates were then used to estimate acute HIV Fiebig stages (a).[47,48] The majority of the cohort was of non-White self-reported race/ethnicity, consistent with national trends for people incident acute HIV (b).[49]

Fig. 2: Semiparametric monophasic, biphasic, and triphasic generalized additive models of HIV reservoir decay during weeks 0-24. We performed bootstrapping to estimate the Akaike information criteria (AIC) value and 95% confidence intervals and compared monophasic, biphasic, and triphasic models for both HIV intact (left panels) and defective (right panels) DNA assays (a). Using the triphasic models for HIV intact (left panel) and defective (right panel) DNA, we then determined the optimal inflection point(s), τ, by minimizing the predicted mean absolute error (MAE; top panels) using leave-one-out cross-validation or the predicted mean squared error (MSE; bottom panels) (b). Red dots denote the optimal inflection point(s), τ, for each model and prediction loss metric. For HIV intact DNA, the first (x-axis) and second (y-axis) inflection points were relatively similar, suggesting that a single inflection point – i.e., a biphasic model – adequately described the data. For HIV defective DNA, the first inflection point (x-axis) was close to zero, this again suggested that a biphasic model reasonably described the data.

Fig. 3 Determination of optimal inflection points for HIV intact and defective DNA biphasic decay models. Using the biphasic models for HIV intact (left panel) and defective (right panel) DNA, we then determined the optimal inflection point(s), τ, by minimizing the predicted mean absolute error (MAE; top panels) using leave-one-out cross-validation or the predicted mean squared error (MSE; bottom panels) (b). An inflection point of τ = 5 weeks (vertical dashed line) best fit decay patterns for both HIV intact (left panels) and defective (right panels) DNA. Red dots denote the best τ for each model and prediction error metric.

Fig. 4 Predicted decay patterns of HIV intact and defective DNA during acute treated HIV from weeks 0-24. Decay patterns for observed (thin grey lines) HIV intact and total defective (a), as well as 3' and 5' defective (b) DNA closely fit with average model predictions (thick black lines). Sampling timepoints are labeled on the x-axis (including a week 2 study visit during which confirmatory HIV test results were disclosed). We estimated average predicted participant decay rates by taking the mean of E_i (estimated time between HIV infection and ART initiation), C_i (initial CD4+ T cell count), and V_i ($\log_{10}$ pre-ART plasma viral load) across participants from final models.

Fig. 5 HIV intact and defective DNA decay patterns were associated with known clinical factors associated with HIV reservoir size. The observed HIV DNA data are shown as thin grey lines for each participant, while the decay pattern for the model-predicted average participant is shown as the thick black lines. Biphasic decay patterns for HIV intact (left panel) and combined defective (3' plus 5', right panel) were faster among participants initiating ART earlier (<30 days vs. 30-100 days) (a), with higher initial CD4+ T cell counts (shown by tertiles) (b), and lower pre-ART viral load (shown by tertiles) (c).

Fig. 6 Predicted HIV intact and defective DNA decay rates, by tertiles of clinical factors associated with HIV reservoir size. We performed bootstrapping to estimate the average predicted decay rates of HIV intact (left panels) and defective (right panels) DNA, stratified by tertiles of known clinical factors associated with HIV reservoir size: timing of ART initiation (a), initial CD4+ T cell count (b), and pre-ART viral load (c).

Supplementary Fig. 1: The UCSF Treat Acute HIV cohort study participants. A total of 67 participants met inclusion criteria for acute HIV, defined as <100 days since the estimated date of detected HIV infection (EDDI) using the Infection Dating Tool (https://tools.incidence-estimation.org/idt/). The numbers of study participants by Fiebig stages (I-V) of HIV recency are also shown (https://doi.org:10.1097/01.aids.0000076308.76477.b8). PrEP = Pre-exposure prophylaxis with tenofovir disoproxil fumarate/emtricitabine (TDF/FTC).

Supplementary Fig. 2: Calculation of estimated dates of detected HIV infection. The estimated dates of detected HIV infection (EDDI), along with a “confidence interval” for early probable (EP-EDDI) and late probable (LP-EDDI) dates, were calculated using participants’ clinical test results as well as baseline study visit confirmatory assay results.

Supplementary Fig. 3: HIV-1/2 test results for study participants. The proportion of study participants with either negative and/or indeterminate test results for HIV-1/2 p24 antigen/antibody assay (Architect) (a) and HIV-1/2 differentiation (Geenius) antibody assay (b) at baseline study visit were consistent with rates with our San Francisco Department of Public Health rates (27% and 28%, respectively).

Supplementary Fig. 4: HIV intact and defective DNA decay patterns by self-reported gender and prior PrEP use. Observed HIV intact and defective DNA data, highlighting the one cisgender female (yellow line) and one transgender female (blue line) participants (a). Participants reporting PrEP use within 10 days of HIV diagnosis fell into two categories: 6 participants who acquired HIV while already taking PrEP (yellow lines), and 8 participants who were found to already have acquired HIV at the time of PrEP initiation (blue lines). All other study participants are shown as grey lines.

Supplementary Fig. 5: Fine tuning of biphasic decay model inflection points from weeks 0-52. A total of 65.7% of the study participants continued in follow-up beyond 24 weeks. We further refined our estimates for the inflection point, τ, by testing sequential half-week windows from 0 to 52 weeks and comparing the minimum prediction error using the leave-one-out mean absolute error (MAE, upper panels) or the leave-one-out mean squared error (MSE, lower panels). An inflection point of τ = 5 weeks (vertical dashed line) remained the best fit decay pattern for both HIV intact (left panels) and defective (right panels) DNA out to 52 weeks of ART. Red dots denote the best τ for each model and prediction error metric.

Supplementary Table 1. Model estimates for HIV intact and defective DNA reservoir decay rates during acute treated HIV. Slope and half-life ($t_{1/2}$) estimates of HIV intact and defective decay rates for unadjusted (a-b) and adjusted models (b-c) during frequently sampled timepoints (weeks 0-24; a, c) and extended out to one year (weeks 0-52; b, d). Adjusted models included covariates for initial CD4+ T cell count, pre-ART HIV RNA, and timing of ART initiation.

Supplementary Fig. 6: Predicted decay patterns of HIV intact and defective DNA during acute treated HIV from weeks 0-52. A total of 65.7% of the study participants continued in

follow-up beyond 24 weeks. Decay patterns for observed (thin grey lines) HIV intact (left panel) and total defective (right panel) DNA closely fit with average model predictions (thick black lines). Sampling timepoints are labeled on the x-axis (including a week 2 study visit during which confirmatory HIV test results were disclosed). Average predicted participant predictions were made by taking the mean of E_i (estimated time between HIV infection and ART initiation), C_i (initial CD4+ T cell count), and V_i ($\log_{10}$ pre-ART plasma viral load) across participants from final models.

Supplementary Fig. 7: Predicted versus observed plots show good model performance for both HIV intact and defective DNA. Validation for the final models for intact and defective HIV DNA decay was initially performed by looking at the plots of predicted vs observed HIV DNA counts. These plots show that both models produce relatively unbiased estimates across the observed range of HIV DNA counts and that the residual variance in the defective reservoir is much higher than the intact reservoir. Red dashed line denotes the idealized fit where predicted values exactly equal observed values.

Supplementary Fig. 8: Sensitivity analyses estimating HIV intact and defective DNA decay rates after excluding potential outlier clinical subgroups. The final model (τ = 5 weeks) was fit on three clinically interesting sub-populations to assess if the influence of potential outlier data. Separate models were fit that excluded (a) participants reporting prior PrEP use (<10 days overlap between last PrEP use and estimated date of detected HIV infection), (b) participants with plasma viral load “blips” (defined as a one-time viral load >1000 copies/mL or two consecutive viral loads >100 copies/mL between weeks 0-24), and (c) participants with sudden increases in HIV intact DNA (defined as >50% increase between two consecutive measurements of HIV intact DNA during weeks 0-24). Models were fit using the cohort data (grey lines), but not the potential outlier data (red lines). The resulting predicted

average participant HIV reservoir decay patterns are shown as thick black lines. Refer to **Supplementary Table 1** to get the sample sizes and half-life estimates for each sensitivity analysis.

Supplementary Fig. 9: Inflection point sensitivity analyses demonstrate some variability when excluding populations of potential outliers. To test whether the final model inflection point selection of $\tau = 5$ weeks was influenced by potential outlier data we performed τ estimation on three clinically interesting sub-populations. Separate models were fit that excluded (a) participants reporting prior PrEP use (<10 days overlap between last PrEP use and estimated date of detected HIV infection), (b) participants with plasma viral load "blips" (defined as a one-time viral load >1000 copies/mL or two consecutive viral loads >100 copies/mL between weeks 0-24), and (c) participants with sudden increases in HIV intact DNA (defined as >50% increase between two consecutive measurements of HIV intact DNA during weeks 0-24). A regular grid of possible τ was used (0-26 weeks by half-week) and the leave-one-out cross-validation (LOOCV) mean absolute prediction error (MAE) was computed for each candidate τ. Red dots denote the best τ for each model and prediction error metric and our selected inflection point ($\tau = 5$) is shown with a dashed vertical line. Refer to **Supplementary Table 1** to get the sample size for each sensitivity analysis and to **Supplementary Fig. 9** to see which patients are excluded from each sensitivity analysis.

Supplementary Table 2. Sensitivity analyses of HIV intact and defective DNA reservoir decay rates during acute treated HIV. Slope and half-life estimates of HIV intact and defective decay rates after excluding participants reporting prior preexposure prophylaxis (PrEP) use within 10 days of estimated date of HIV infection (a), participants with plasma viral load "blips" (defined as a one-time viral load >1000 copies/mL or two consecutive viral loads >100

copies/mL between weeks 0-24) (b), and participants with sudden increases in HIV intact DNA (defined as >50% increase between two consecutive measurements of HIV intact DNA during weeks 0-24) (c). All models were adjusted for initial CD4+ T cell count, pre-ART HIV RNA, and timing of ART initiation.

Supplementary Table 3. The effect of earlier ART initiation on HIV intact and defective DNA decay rates. We performed bootstrapping to calculate the difference in half-life estimates for HIV intact and defective DNA, with each week that ART is initiated earlier. All models were adjusted for initial CD4+ T cell count and pre-ART HIV RNA.

Supplementary Table 4. The effect of higher initial CD4+ T cell count or lower pre-ART HIV RNA on HIV intact and defective DNA decay rates. We performed bootstrapping to calculate average half-life estimates for HIV intact and defective DNA for each quartile change in initial CD4+ T cell count or pre-ART HIV RNA. Models estimating the effect of initial CD4+ T cell count were adjusted for timing of ART initiation and pre-ART HIV RNA. Models estimating the effect of pre-ART HIV RNA were adjusted for timing of ART initiation and initial CD4+ T cell count.

Supplementary Fig. 10: Fitted spline models to estimate the effect of higher initial CD4+ T cell count or lower pre-ART HIV RNA on HIV intact and defective DNA decay rates. Fitted spline models (red lines) with corresponding 95% confidence intervals (blue dashed lines) are shown for HIV intact DNA (a) and HIV defective (b) DNA. Plots are shown for pre-ART HIV RNA (left panels) and initial CD4+ T cell count (right panels).

Supplementary Fig. 11: Semiparametric monophasic, biphasic, and triphasic generalized additive models of plasma HIV RNA decay during weeks 0-24. We performed bootstrapping

458 to estimate the Akaike information criteria (AIC) value and 95% confidence intervals and
459 compared monophasic, biphasic, and triphasic models for plasma HIV RNA (a). Using the
460 triphasic model for plasma HIV RNA, we then determined the optimal inflection point(s), τ, by
461 minimizing the predicted mean absolute error (MAE; top panel) using leave-one-out cross-
462 validation or the predicted mean squared error (MSE; bottom panel) (b). Red dots denote the
463 optimal inflection point(s), τ, for the model and loss metric. These analyses demonstrated an
464 inflection point at 0.5 weeks (red dot at x-axis) and 4 weeks (red dot at y-axis), suggesting that a
465 triphasic model best fit the data (b).
466
467 **Supplementary Table 5. Model estimates of plasma HIV RNA decay rates during acute**
468 **treated HIV.** Slope and half-life ($t_{1/2}$) estimates of plasma HIV RNA decay rates for models
469 adjusted for initial CD4+ T cell count and timing of ART initiation during frequently sampled
470 timepoints (weeks 0-24). Models included a random intercept for each participant. We
471 calculated estimates for each phase of the final triphasic decay model: 0 to 0.5 weeks, 0.5-4
472 weeks, and 4-24 weeks. We did not observe a statistically significant decay of plasma HIV RNA
473 after week 4, given that the majority of participants had undetectable plasma HIV RNA levels
474 after a median of 4.14 weeks on ART.
475
476 **Supplementary Fig. 12: Predicted versus observed plots demonstrating model**
477 **performance for plasma HIV RNA**. Validation for the final model for plasma HIV RNA decay
478 was initially performed by looking at the plots of predicted vs observed plasma HIV RNA counts.
479 This plot shows that the triphasic model produces unbiased estimates for a large range of
480 plasma HIV RNA counts. The model systematically underestimates very large plasma HIV RNA
481 values and has high variability at very low plasma HIV RNA values (e.g., <40 copies/mL). Red
482 dashed line denotes the idealized fit where predicted values exactly equal observed values.

Supplementary Fig. 13: Plasma HIV RNA decay patterns were associated with known clinical factors associated with HIV reservoir size. The observed plasma HIV RNA data are shown as thin grey lines for each participant. Plasma HIV RNA decay was faster among participants initiating ART earlier (<30 days vs. 30-100 days) (a) and with higher initial CD4+ T cell counts (shown by tertiles) (b).

Supplementary Fig. 14: Predicted plasma HIV RNA decay rates, by tertiles of clinical factors associated with HIV reservoir size. We performed bootstrapping to estimate the average predicted decay rates of plasma HIV RNA, stratified by known clinical factors associated with HIV reservoir size: timing of ART initiation (a) and initial CD4+ T cell count (b).

Supplementary Fig. 15: Fitted spline models to estimate the effect of higher initial CD4+ T cell count on plasma HIV RNA decay rate. Fitted spline model (red line) with corresponding 95% confidence interval (blue dashed line) is shown for plasma HIV RNA in relation to initial CD4+ T cell count.